Dinuclear Cu(I) Halides with Terphenyl Phosphines: Synthesis, Photophysical Studies and Catalytic Applications in Cu-AAC Reactions

Álvaro Beltrán,[†] Inmaculada Gata,[†] Celia Maya,[‡] João Avó,[§] João Carlos Lima,[#] César A. T. Laia,[#] Riccardo Peloso,*,[‡] Mani Outis*,[#] and M. Carmen Nicasio*,[†].

†Departamento de Química Inorgánica, Universidad de Sevilla, Aptdo 1203, 41071 Sevilla, Spain

‡Instituto de Investigaciones Químicas (IIQ), Departamento de Química Inorgánica and Centro de Innovación en Química Avanzada (ORFEO-CINQA), Consejo Superior de Investigaciones Científicas (CSIC) and Universidad de Sevilla, Avenida Américo Vespucio 49, 41092 Sevilla, Spain

§ IBB-Institute for Bioengineering and Biosciences, Instituto Superior Técnico, Universidade de Lisboa, 1049-001 Lisboa, Portugal.

#LAQV-REQUIMTE, Departamento de Química, Faculdade Ciências e Tecnologia, Universidade NOVA de Lisboa, 2829-516 Monte de Caparica, Portugal.

ABSTRACT: Several dinuclear terphenyl phosphine copper(I) halide complexes of composition $[CuX(PR_2Ar')]_2$ (X = Cl, Br, I; R = hydrocarbyl, Ar' = 2,6-diarylterphenyl radical), **1-5**, have been isolated from the reaction of CuX with 1 equiv of the phosphine ligand. Most of them have been characterized by X-ray diffraction studies in the solid state, thus allowing comparative discussions of different structural parameters, namely Cu···Cu and Cu···Aryl separations, conformations adopted by coordinated phosphines, planarity of the Cu_2X_2 cores. Centrosymmetric complexes $[CuI(PMe_2Ar^{Xyl2})]_2$, **1c** and $[CuI(PEt_2Ar^{Mes2})]_2$, **3c**, despite their similar structures, show very distinct photoluminescence (PL) in powder form at room temperature. The photophysical behavior of these compounds in liquid solution, solid-solid Zeonex solution and powder samples at room temperature and 77 K have been investigated and supported by DFT calculation. Identification of vibronic coupling modes, done by group theory calculations and the technique of projection operators, shows that the manifestation of these modes is conditioned by crystal packing. Complexes $[CuI(PMe_2Ar^{Xyl2})]_2$, **1c** and $[CuI(PEt_2Ar^{Mes2})]_2$, **3c** display remarkable activity in copper-catalyzed azide-alkyne cycloaddition reactions involving preformed and in situ-made azides. Reactions are performed in H_2O, under aerobic conditions, with low catalyst loadings and tolerate the use of iodoalkynes as substrates.

INTRODUCTION

Cu(I) halides with phosphines display a variety of coordination numbers and geometries primarily dictated by the size of the phosphine and, to a lesser degree, by the nature of the halide.[1] Thus for a 1:1 stoichiometry, tetranuclear $[CuX(PR_3)]_4$ with cubane-like structure, are frequently encountered for less bulky phosphines such as PEt_3,[2] PMe_2Ph[3] and PPh_3.[4] Furthermore, for the larger halides (Br and I)[5] less common stepped cubane structures have also been found. As the size of phosphine increases, dinuclear $[CuX(PR_3)]_2$ species with three-coordinate Cu(I) centers are stabilized, as noted for PCy_3,[6] $P(o\text{-Tol})_3$,[7] PBz_3,[8] (Bz = benzyl) among others.[9] Mononuclear two-coordinate $[CuX(PR_3)]$ are obtained for the highly sterically demanding phosphines $PMes_3$[10] (Mes = mesityl) and $P(tmp)_3$ (tmp = 2,4,6-trimethoxyphenyl).[11]

Due to their flexible coordination properties, Cu(I) halides aggregates have been incorporated, as building blocks, in coordination polymers,[1,12] which exhibit a range of photophysical properties.[13] In this context, discrete $\{Cu_nI_n\}$ clusters display interesting properties such as polymorphism, thermochromism and thermally activated delayed fluorescence (TADF).[14-17] Concerning the
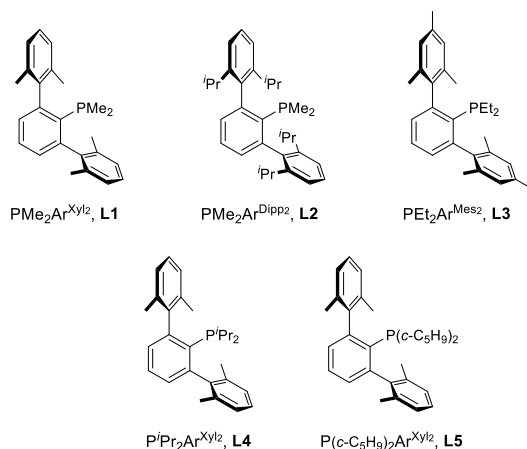
Relativistic Nephelauxetic Effect through covalent character of Cu-I, bonds and large spin-orbit coupling (SOC) constant of I[18], a remarkable advantage of these compounds can be thought as conferring heaviness to a light metal based core. First row (3d) transition metals are not heavy enough for an efficient SOC but, a high SOC is required for rapid Inter-System-Crossing (ISC) in order to achieve phosphorescent metal complexes. Third row (5d) transition metal based complexes like those of Ir(III) and Pt(II) exhibit the desirable fast ISC as a high SOC is induced by the heavy metal centre itself. These phosphorescent complexes have been the focus of many investigations especially for organic light emitting diodes (OLEDs)[19,20] .However these are very expensive metals and their sources are increasingly scarce. Thus, luminescent Cu(I) halides aggregates represents an attractive sustainable alternative to those based on heavy precious metals.

Additionally, Cu(I) complexes enjoy a rich catalytic chemistry, including cross-coupling reactions,[21] oxidations,[22] borylation reactions,[23] C-H functionalization[24] and 1,3-dipolar cycloadditons, in particular, the Cu-catalyzed Azide-Alkyne Cycloaddition (Cu-

AAC).[25] The latter is the most prominent example of click chemistry.[26] Nitrogen-containing ligands and N-heterocyclic carbenes, albeit to a lesser extent, have commonly been used as supporting ligands in CuAAC reactions.[25,27] However, Cu(I) complexes stabilized by phosphine ligands have scarcely been applied.[28] Recently, Díez-González and co-workers have employed mononuclear and tetranuclear Cu(I) halides bearing phosphorus(III) ligands as catalysts in efficient CuAAC reactions performed in water under mild conditions.[29]

We have developed a family of heteroleptic phosphine ligands bearing a bulky terphenyl substituent, PR_2Ar' (Ar' = terphenyl radical) (Chart 1) and we have evaluated their electronic and steric parameters.[30,31] Herein, we report on the synthesis and structures of a series of dinuclear $[CuX(PR_2Ar')]_2$ complexes. Two new phosphorescent complexes containing the Cu_2I_2 core have been identified and their excited state dynamics where low-lying electronic transitions are mainly (M+X)LCT are discussed. In addition, the catalytic activity of these complexes in CuAAC reactions is also examined.

Chart 1. Terphenyl phosphines used in this work.

PMe$_2$Ar^{Xyl2}, **L1** PMe$_2$Ar^{Dipp2}, **L2** PEt$_2$Ar^{Mes2}, **L3**

P^{i}Pr$_2$Ar^{Xyl2}, **L4** P(c-C$_5$H$_9$)$_2$Ar^{Xyl2}, **L5**

RESULT AND DISCUSSION

Synthesis and structural studies of Cu(I) Complexes. Dinuclear complexes 1-5, of the general formula CuX(PR$_2$Ar') (PR$_2$Ar' = **L1**, X = Cl, Br, I: **1a, 1b, 1c**; PR$_2$Ar' = **L2**, X = Cl, Br, I: **2a, 2b, 2c**; PR$_2$Ar' = **L3**; X = Cl, Br, I: **3a, 3b, 3c**; PR$_2$Ar' = **L4**, X = I: **4c**; PR$_2$Ar' = **L5** X = Cl, Br, I: **5a, 5b,5c**) were synthesized by mixing equimolar amounts of the corresponding copper(I) halide, CuX, and the dialkyl terphenyl phosphine, PR$_2$Ar', in dichloromethane at room temperature. The transformation of the metal precursor into the product occurred with concomitant disappearance of the colorless copper halide, which was almost insoluble in the reaction medium. Reaction times of about 12 h were required to achieve high yields.

Compounds 1-5 were isolated as air-stable colorless solids. They are highly soluble in chlorinated and aromatic solvents and poorly soluble in saturated hydrocarbons such as pentane, heptane, or petroleum ether. ^{31}P{^{1}H} NMR spectra of complexes 1-5 revealed that the broad resonances of the P nuclei are slightly or moderately shifted to higher frequencies ($\Delta\delta$ ca. 0.5 to15 ppm)

upon coordination to the metal center, analogously to what observed for related Ni,[31] Pt, Rh, Ir,[30] and Au[32] compounds. The ^{1}H NMR and ^{13}C{^{1}H} NMR spectra of CuX(PR$_2$Ar) species in CDCl$_3$ do not show any relevant differences compared to the free ligands, which is consistent with a monodentate coordination mode of the P ligand in conjunction with fast rotations around the P–Cu and/or P–C$_{aryl}$ bonds. Nevertheless, the previously observed κ^1-P,η^1-C coordination of the terphenyl phosphine[30-32] cannot be ruled out in solution, given that a fast interchange of the two flanking aryl rings of the terphenyl group in the coordination environment of the metal would also account for the observed NMR properties. If only mononuclear and dinuclear complexes are considered, four possible structures in solution can be envisaged (Fig 1).
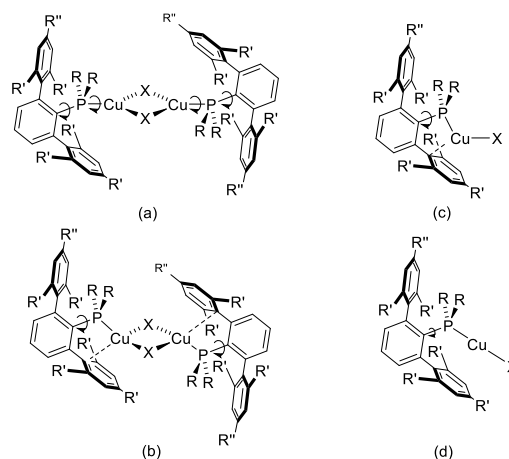

Figure 1. Possible coordination modes of PR$_2$Ar' ligands and geometries around the Cu centre for mononuclear and dinuclear CuX(PR$_2$Ar') species in solution based on NMR data. Arrows indicate fast rotations on the NMR time scale. (a) κ^1-P monodentate coordination, dinuclear, trigonal planar geometry at Cu; (b) κ^1-P,η^1-C bidentate coordination, dinuclear, tetrahedral geometry at Cu; (c) κ^2-P,C bidentate coordination, mononuclear, trigonal planar geometry at Cu; (d) κ^1-P monodentate coordination, mononuclear, linear geometry at Cu.

DOSY ^{1}H NMR experiments of CDCl$_3$ solutions of complexes **1c, 2a, 3c** and **5b** were performed in order to get more information about the nuclearity of the CuX(PR$_2$Ar') species in solution (see Figure 1 in SI). In all cases only one species was detected with calculated diffusion coefficients of *ca.* 6-7·10^{-10} m^2·s^{-1}, in accord with previously reported data for complexes of similar size.[33] Moreover, the diffusion coefficients were used to calculate the corresponding hydrodynamic radii of the molecules with the Stokes-Einstein equation giving values of *ca* 6-7 Å in good agreement with the equivalent radii estimated from the X-Ray molecular structures of the dimers.

X-ray diffraction analyses were conducted on single crystals of complexes **1, 2c, 3b, 3c, 4c, 5c**, revealing that their molecular structures in the solid consist in bimetallic dihalo-bridged neutral complexes, $[Cu(\mu-X)(PR_2Ar')]_2$, with the metal centers lying in a distorted trigonal planar geometry. This type of complex has numerous precedents in the literature.[6-9] ORTEP diagrams

Table 1. Selected structural parameters for $[Cu(\mu-X)(PR_2Ar')]_2$ complexes 1-5 in the solid state.

Complex	X	R	Ar'	Cu-Cu (Å)	Cu-X-Cu (°)	[Cu$_2$X$_2$] planarity	Cu-Ar (shortest Cu-C)	Sum of bond angles at Cu	Point group*	Conformation of PR$_2$Ar'
1a	Cl	Me	Ar^{Xyl2}	3.04	82[a]	no	2.76	356	C$_1$	A and C
1b	Br	Me	Ar^{Xyl2}	2.88	73[a]	no	2.86[a]	352	C$_s$ (C$_1$)	C
1c	I	Me	Ar^{Xyl2}	2.62	60.7	yes	2.96	352	C$_{2h}$(C$_i$)	C
2c	I	Me	Ar^{Dipp2}	2.69	63[a]	no	3.20[a]	354[a]	C$_s$ (C$_1$)	B
3b	Br	Et	Ar^{Mes2}	3.15	80.4	yes	2.83	353	C$_{2h}$(C$_i$)	C
3c	I	Et	Ar^{Mes2}	3.35	80.5	yes	2.90	352	C$_{2h}$(C$_i$)	C
4c	I	iPr	Ar^{Xyl2}	3.12	73.7	yes	3.82	354	C$_{2h}$(C$_i$)	C
5c	I	Cyp	Ar^{Xyl2}	3.90	90.0	yes	2.69	352	C$_{2h}$(C$_i$)	C

[a]Mean.

*Symmetry of the [CuX(PR$_2$Ar')]$_2$ complexes reached after slight rotation of the aryl groups around the P-C$_{ipso}$ and C-C axis and/or translations of the X ligands (point group found in the X-ray structure). See discussion.
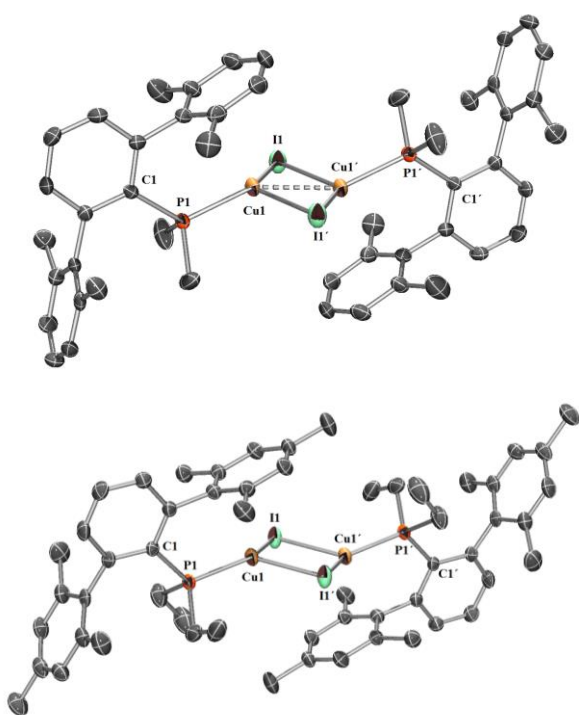

Figure 2. ORTEP views for the molecular structures of complexes **1c** (top) and **3c** (bottom). Selected bond distances (Å) and angles (°) for **1c**: Cu1-P1 2.2171(9), Cu1-I1 2.5853(5), Cu1-I1´ 2.5886(5), Cu1-Cu´ 2.6175(6), Cu1-I1-Cu1´ 60.78(1), P1-Cu1-I1 115.03(3), P1-Cu1-I1´ 117.55(3), I1-Cu1-I1´ 119.22(2).; for **3c**: Cu1-P1 2.217(1), Cu1-I1 2.6125(5), Cu1-I1´ 2.5795(6), Cu1-I1-Cu1´ 80.45(2), P1-Cu1-I1 126.60(3), P1-Cu1-I1´ 126.97(3), I1-Cu1-I1´ 99.55(2).

for the molecular structures of complexes **1c** and **3c** are depicted in Fig. 2 as representative examples.

Interestingly, for all structures, the slightly pyramidalized copper atoms lie at ca. 0.3-0.4 Å above the plane defined by the two halides and the P atom and points towards one of the lateral rings of the terphenyl group. This observation may suggest the existence of week bonding interactions, reasonably of electrostatic nature, between the copper centre and one or two carbon atoms of the aromatic rings, especially for complexes **1a** and **5c**, which exhibit the shortest Cu···C$_{aryl}$ separations (ca. 2.7 Å). Based on the comparison of the Cu···C$_{aryl}$ distances reported in Table 1 with the sum of the covalent radii of C(sp^2) and Cu (ca. 2.0 Å),[34] the existence of "classical" copper-carbon covalent bonding is ruled out clearly. For the sake of comparison, the extent of copper-carbon interactions in complexes **1-5** appears

much smaller than in related unsaturated platinum complexes [PtMe(OH$_2$)(PMe$_2$Ar^{Dipp2})]$^+$,[30b] [PtMe$_2$(PMe$_2$Ar^{Dipp2})]$^+$,[30b] [PtCl$_2$(PMe$_2$Ar^{Dipp2})]$^+$,[30a] and [Pt(tBuCH=CH$_2$)(PMe$_2$Ar^{Dipp2})],[30c] in which shorter Pt···C$_{aryl}$ metal-carbon separations of ca. 2.2-2.3 Å are observed. Another point of interest of the structural properties of complexes **1-5** is the existence, in some cases, of typical d^{10}-d^{10} interactions[35] resulting in Cu—Cu separations of approximately 2.6-2.7 Å. For the iodide complexes **1c** and **2c**, which contain the dimethyl phosphines PMe$_2$Ar^{Xyl2} **L1** and PMe$_2$Ar^{Dipp2} **L2**, the Cu—Cu distance matches almost perfectly the double of the covalent radius of copper (1.32 Å),[34] thus indicating a clear Cu(I)-Cu(I) bond. The correlation between the metal-metal separation and the CuXCu bond angle for complexes **1-5** is plotted in Figure S8 (see Supporting Information), and discloses a fair linear dependence, particularly for acute angles. In general, R substituents in PR$_2$Ar' bulkier than CH$_3$ seem to impede the formation of a metal-metal bond, reasonably for steric reasons, with copper-copper separations larger than 3 Å.

The solid state structures of complexes **1-5** deserve some additional comments on their molecular symmetry and the conformation of the dicopper [Cu$_2$X$_2$] cores and the phosphine ligands. Although most of the [Cu(μ-X)(PR$_2$Ar')]$_2$ species studied in this work show C$_i$ symmetry (C$_1$ in three cases), by slight rotations of the aryl rings around the C—C and P—C bonds and slight translations of the X ligands for non-planar [Cu$_2$X$_2$] cores, a C$_{2h}$ symmetry would be easily reached. Figure 3 provides a schematic representation of the C$_{2h}$-like molecular structure and the symmetry elements showed by the majority of [Cu(μ-X)(PR$_2$Ar')]$_2$ dimers in an idealized geometry.
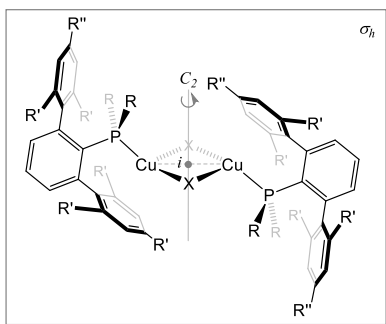
Figure 3. C$_{2h}$-like molecular structure and the symmetry elements in most of the [Cu(μ-X)(PR$_2$Ar')]$_2$ dimers described in this work.

The conformations adopted by the terphenyl phosphines used in this work have recently been analyzed by some of us.[31] Three possible conformations have been identified (Figure 4), being the type C the most common by far in the dicopper complexes of this work. This observation could reasonably be explained by the existence of some Cu⋯C interaction. Anyway, taking into account that the NMR spectra of all complexes are consistent with fast rotations around the P—Cu and/or P—C bonds, the energy separations between the different conformations in solution are likely small. The neutral [Cu$_2$X$_2$] cores are planar or quasi-planar (deviations from the middle plane less than 0.13 Å) with no apparent relation with other metric parameters.
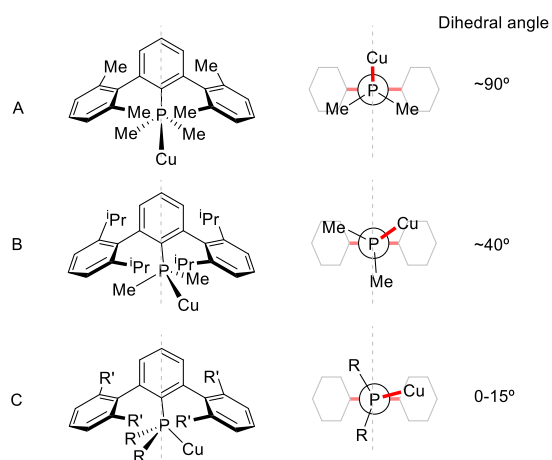

Figure 4. Conformations observed in the solid state by the Cu-coordinated terphenyl phosphines PR$_2$Ar' used in this work

Photophysical Studies. The nature of transitions within a sole isolated molecule can be assigned through UV-Vis spectra of complexes **1c** and **3c** as well as the spectra of their corresponding free ligands shown in Fig. 5. The complexes display an additional electronic transition at longer wavelengths (above 300 nm) assigned to Metal and Halide to Ligand Charge Transfer band ((M+X)LCT), which has been confirmed with TD-DFT calculations (see below). Intra-ligand electronic transitions are observed at lower wavelengths in the complexes, matching the observed transition in the UV-Vis spectra of the respective free ligands.

The photoluminescence (PL) of **1c** and **3c** is negligible in solution at room temperature, even in degassed conditions. Thus, to allow the characterization of their optical properties, the PL of

these complexes must be studied in solid state (powder, dispersion in polymer matrix and in frozen solution at 77K).

Both complexes are emissive in powder solid phase, however they display different features at different temperatures. At 77 K the excitation and emission spectra of both complexes are very similar (Fig. 6). At room temperature, the emission band of **3c** becomes slightly broader without significant change of its emission maximum with Φ$_L$ of 19%, while **1c** has only very residual emission. The diffuse reflectance of powder samples with Kubelka-Munk transformation function f(r∞) are shown in Fig. 6, which exhibits barely resolved absorption bands at 285 nm and 335 nm coincident with the excitation and UV-Vis bands in solution. This same position confirms the localization of the excitation and thus emission from isolated molecules.[36]
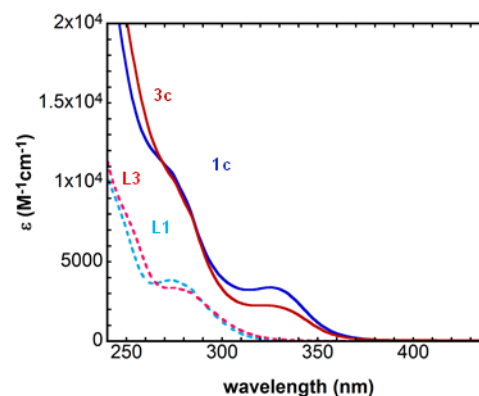

Figure 5. UV-Vis spectra of complexes **1c** and **3c** (bold line) and their corresponding free ligands (dashed line) in cyclohexane.
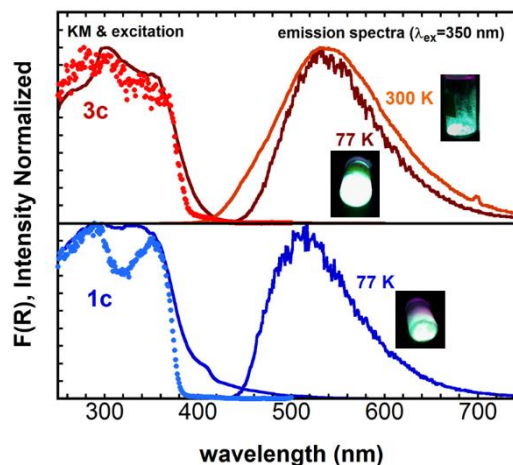
Figure 6. Diffuse Reflectance spectra of the complexes under Kubelka-Munk (KM) transformation function (f(r∞)bold lines) overlapped with the excitation spectra at 77 K collected at 515 nm for **1c** and at 525 nm for **3c** (pointed lines). Emission spectra of powder samples excited at 350 nm at 77 K and 300 K .

As isolated molecules can indeed be emissive in solid state, we did the characterization also in Zeonex solid-solid solution at room temperature. In this rigid matrix, at room temperature, **1c** and **3c** display almost identical spectral behaviour (Fig. 7) as those found for powder samples at 77 K. This behaviour discards

the possibility of aggregation induced emission. Room temperature decay time measurement performed on films placed in vacuum exhibit a mono-exponential decay with lifetime of 56 μs for **1c** and 82 μs for **3c** (Fig. S9 in SI). In air saturated environment one can clearly notice the quenching effect of O$_2$. The long life time and the sensitivity to oxygen strongly suggest that luminescence arises from excited triplet states.
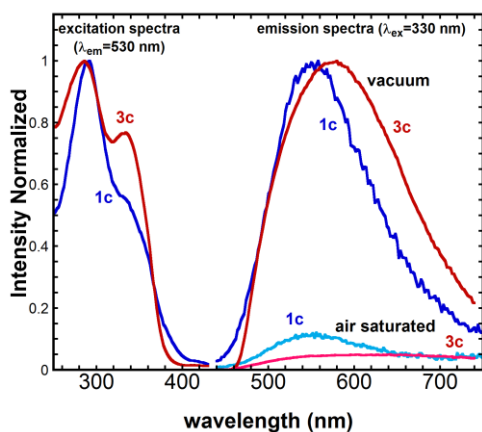
Figure 7. Excitation and Emission spectra of complexes **1c** and **3c** in solid film dispersion in vacuum and in the presence of air.

The narrowing of the emission band at 77 K without a noticeable shift of observed emission (Fig 6 top) and the large Stokes shift (ca. 1.42 eV) is compatible with the assignment of the observed emission to phosphorescence from lower triplet state. For a better understanding of the emission properties a deeper analysis with theoretical calculations using TD-DFT were carried out.

TD-DFT calculations. Calculated excitation energies for optimized geometries in cyclohexane are in good agreement with the experimental UV-Vis spectra (Fig S10 in SI). TD-DFT calculations reveal an essentially (M+X)LCT character of low-lying electronic transitions with some contribution of Intra-Ligand Charge transfer (ILCT) through participation of P atoms. In both **1c** and **3c** which are centrosymmetric complexes, the S$_1$ state would be achieved by a mainly HOMO→LUMO transition, forbidden by Laporte symmetry selection rule (u→u). However the S$_2$ state is reached by a mainly HOMO→LUMO+1, which is a symmetry allowed transition (u→g). DFT calculations show also that LUMO and LUMO+1 are degenerate molecular orbitals (Fig. 8).
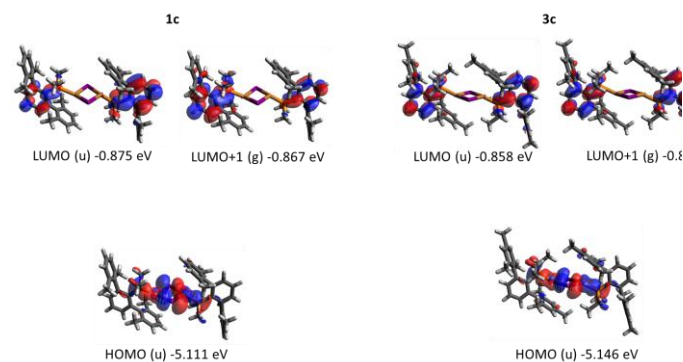
Figure 8. Frontier Orbitals, their respective parity and energies. LUMO and LUMO+1 are degenerated Molecular Orbitals.

These theoretical results confirms that once the molecule achieves the excited state any Internal-Conversion (IC) from S$_2$ to S$_1$ would lead to a non-radiative decay path as S$_1$ to S$_0$ is a forbidden transition. So the population of the triplet manifold should be done upon ISC from S$_2$. In both cases the closest triplet state in energy is T$_8$ which is of mainly (HOMO,LUMO+1) configuration as like as S$_2$ (Table 2). The same configuration of S$_2$ and T$_8$ has important consequences: (i) a very small energy gap between the two charge transfer states due to decreased exchange integral between the unpaired electrons; (ii) same electronic configuration does not involve different type of orbitals thus ISC between them would be weak via vibronic Spin-Orbit-Coupling.[37] However, it is expectable that ISC from S$_2$ to the nearly isoenergetic T$_8$ state could be performed due to the Internal Heavy Atom Effect of Iodine acting on the unpaired electron of HOMO centred on Cu$_2$I$_2$ moiety so that $\langle S_2 | \hat{H}_{SO} | T_8 \rangle \neq 0$.[38]

Table 2. Electronic configuration of first, second Singlet excited state and the closest Triplet state in energy as well as the main involved Molecular Orbitals (f and E are the calculated oscillator strength and excitation energy respectively).

Complex	State	f	E (nm)	MO (%)
1c	S1	0.0008	339	HOMO→LUMO (80%)
	S2	0.0078	338	HOMO→LUMO+1(79%)
	T8	-*	340	HOMO→LUMO+1(20%)
3c	S1	0.0000	335	HOMO→LUMO (92%)
	S2	0.0080	334	HOMO→LUMO+1(92%)
	T8	-*	339	HOMO→LUMO+1(80%)

* N/A as calculations were done without SOC inclusion.

The density of the triplet manifold in the sense of spatial character can be discussed as well. In the case of complex **3c**, 80% of the closest triplet state to S$_2$ is (HOMO,LUMO+1) in configuration interaction. In the case of the complex **1c**, however, the (HOMO,LUMO+1) contribution is just 20% but there are other T$_n$ (n<8) very close in energy one to each other which also have some contribution of (HOMO,LUMO+1) in their configuration interaction set (Table S3 in SI).

Quantum Mechanical properties of these systems like the participation of atomic p orbitals of I in the lowest charge transfer state and small ΔE$_{ST}$ explain the ISC and the experimentally observed phosphorescence. Computational results show that ISC from the initially Franck-Condon (FC) region after excitation is possible without considerable structural change of the excited molecule. Given the spatial character of nearly degenerate charge transfer states the ISC rate constant is expected not to be large enough to be dominant over other possible competitive pathways,[38a] namely $S_2 \overset{ISC}{\rightarrow} T_8$ *versus* $S_2 \overset{IC}{\rightarrow} S_1$. Although it is quite logical to accept that ISC from S$_2$ to triplet manifold is favoured in rigid media as in this kind of environments vibronic couplings responsible for IC from S$_2$ to S$_1$ would be more hindered, this type of analysis of the configuration of the excited states does not explain why powder samples of **1c** are not emissive at room temperature. Our DFT calculations provide further useful information regarding Molecular Orbital energy levels. Accordingly, LUMO and LUMO+1

are quite close in energy, the energetic difference between them being 0.008 eV for **1c** and 0.001 eV for **3c**, close enough to be considered degenerate in both cases. Despite of degeneracy we have treated LUMO and LUMO+1 individually and not as a pair because by symmetry operations of the C_{2h} point group they cannot be transformed into each other or any linear combination of them. Moreover, LUMO and LUMO+1 have different parities (Fig. 8) so, although they are automatically orthogonal Molecular Orbitals of the same kind, they do not have the same symmetry ($\langle \pi_u^* | \pi_g^* \rangle = 0$) and cannot transform as an E type irreducible representation (irrep).[39] Almost simultaneous transition to two potential energy surfaces S_1 and S_2 (Table 2) means vertical transition corresponds to a molecular geometry point where these states are nearly degenerate. So a conical intersection (CI) between S_1 and S_2 within the FC region can be expected. S_1 and S_2 have ^1B_g and ^1A_u symmetries respectively so the degeneracy we are looking for would be between states which belong to different irreps of the same Abelian point group. In this case the CI is not required by symmetry, as in the Jahn–Teller case, but occur rather due to the nature of the two electronic states involved and shall be considered an accidental intersection case.[40] Unlike homoleptic $[Cu(N^\wedge N)_2]^+$ complexes which exhibit flattening Jahn-Teller distortion[41] in these three-coordinate systems pseudo Jahn-Teller effect cannot be expected. The excited state of the heteroleptic dinuclear complexes **1c** and **3c** is formed by promotion of an electron from HOMO which mainly corresponds to the Cu_2I_2 moiety (Fig. 8). Due to the highly covalent character of Cu-I bonds on the one hand and great participation of iodine atoms in HOMO on the other, it is not plausible to assume a pure d^9 configuration for any Cu centres of the $[Cu_2I_2]^+$ core. However, in three coordinated Cu(I) complexes the possibility of other types of distortion in the excited state cannot be ruled out.[42]

The existence of a CI between the optically allowed $S_2(^1A_u)$ and the dark $S_1(^1B_g)$ in the vicinity of the FC zone helps us to postulate a more accurate mechanism of luminescence. We already saw that the ground state geometry of both **1c** and **3c** belong to the C_{2h} abelian point group and does not contain degenerate irreps, but upon vertical excitation a degenerate electronic state is imposed. As mixing between electronic states along nuclear displacements become significant at near degeneracy critical geometries, the excited molecules at FC zone (from which ISC would occur) can undergo non-adiabatic transition from S_2 to S_1 through vibronic coupling.[43a-b] More importantly since the geometry corresponding to the CI is not expected to be quite different from that at FC point, electronic coupling around the CI point can be approximated by low-order expansion around the FC geometry.[43b-c] In this way nuclear dynamics occurring within the S_1-S_2 can be approached as a pairwise interacting states by the well-established Linear Vibronic Coupling (LVC) model. In LVC model the symmetry of the vibrational coordinates that couple electronic states of an Abelian point group is determined by the direct product of the irreps of the electronic states.[40a,43a] In our case the interstate vibronic coupling between S_1 and S_2 will not vanish when the coupling modes are of b_u symmetry as $B_g \otimes A_u = B_u$.

Taking FC point as reference geometry is a very useful approximation making us possible to figure out how these coupling modes would look like. To do so let us focus on dimeric coordination sphere with 6 atoms $[Cu_2I_2(P)_2]$ for the sake of simplicity.

By group theory calculation it is known that among twelve (3N-6) internal coordinates in C_{2h} point group, four of them will be b_u non-totally symmetric odd normal modes. Using the technique of projection operators and being aware of the presence of the Cu_2I_2 four-membered ring[44] one can determine how these symmetry adapted vibrational normal modes look like (Fig. 9).
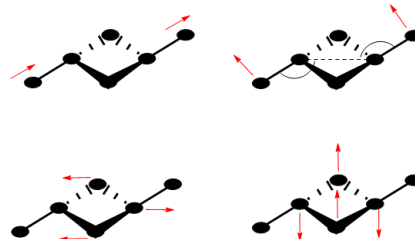

Figure 9. Four vibrational modes of b_u symmetry : asymmetric P-Cu stretching and P^(Cu-Cu) bending (top) Cu_2I_2 in plane ring deformation and out of plane ring puckering (bottom),.

These Group Theory results can explain why unlike other rigid media, in room temperature powder solid phase the PL behavior of **1c** and **3c** is so different. Complexes **1c** and **3c** interact distinctly with adjacent molecules through short contacts. In **3c** there are short contacts stablished through Iodine atoms so the Cu_2I_2 core is somehow stuck within the crystalline network while short contacts through Iodine feature is not present in **1c** (Fig. S11 in SI) and thus individual molecules at 300 K have enough space and flexibility to undergo Cu_2I_2 ring deformation breaking down the geometry at FC zone which the molecule needs to undergo ISC and emit light. The packing force is strong enough to block this deactivating vibrational modes significantly as in the Raman spectra one can notice a characteristic resolved band at 126 cm^{-1} observable in **1c** but not clear in the spectrum of **3c**. The 126 cm^{-1} wavenumber is consistent with the Cu-I stretching in Raman spectroscopy[45] and by the other hand this band is not observable in the free ligands so we can assign it to some Cu-I stretching in **1c**. Although it can correspond only to an even stretching mode (a_g or b_g), experimental evidence of the flexibility of Cu_2I_2 core conditioned by solid state packing is presented by Raman Spectroscopy. (Fig. 10).
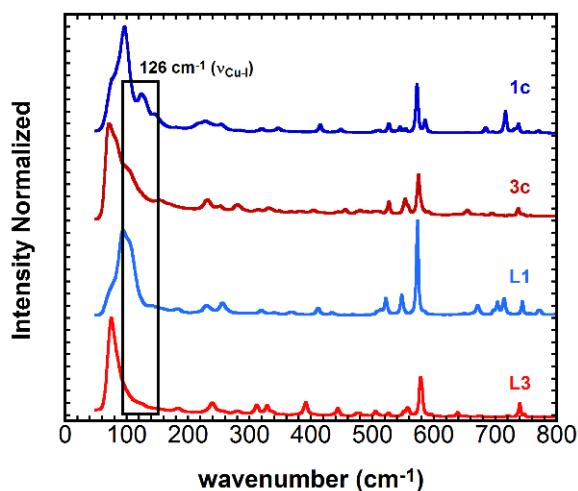

Figure 10. Raman spectra of **1c** and **3c** compared to their corresponding free ligands **L1** and **L3** in order to confirm the assignment of the resolved band at 126 cm^{-1} to Cu-I stretching mode.

Based on spectroscopic observations supported by theoretical calculations we suggest a mechanism of luminescence (Fig. 11). According to this scheme the FC geometry of the ^{1}(M+X)LCT excited molecule should be maintained in order to populate the bright ^{3}(M+X)LCT state. Otherwise distortions namely Cu_2I_2 ring deformation, act as a non-radiative path at the Conical Intersection point which corresponds to photochemical funnel between S_2 and dark S_1.
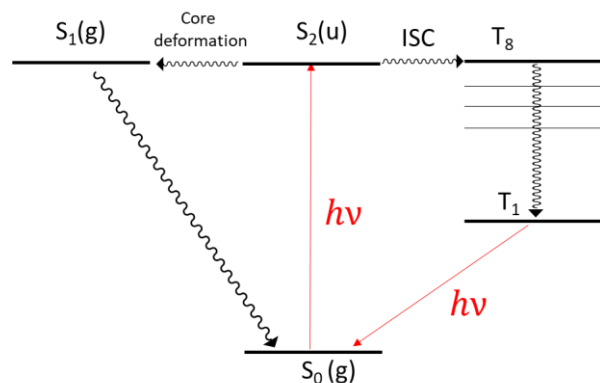

Figure 11. Radiative transitions (red arrows) and non-radiative transitions (curvy arrows) involved in the suggested mechanism of phosphorescence.

The suggested mechanism can explain the photophysical behaviour in deaerated solution where emission quenching is independent of oxygen concentration. While at room temperature none of the two complexes is emissive, in frozen solution at 77 K the spectral behaviour of both **1c** and **3c** is almost identical to those of other rigid media (Fig. S12 in SI). So the quenching of phosphorescence in these complexes can be attributed to their geometrical flexibility in solution rather than specific interactions with solvent molecules.

Catalytic Studies. A survey on the catalytic properties of complexes **1-5** in the CuAAC reaction between benzyl azide and phenyl acetylene, the model reaction, was accomplished. The trials were conducted using the reaction conditions optimized by Díez and co-workers[29] for the catalyst CuBr(PPh$_3$)$_3$, namely, using water as the solvent and 0.5 mol% [Cu] catalyst loading under air. As shown in Table 3, all catalysts tested proved to be active in the model system under these conditions. However, those with the less bulky phosphine ligands (**L1** and **L3**) displayed the best activities (entries 1-3 and 6-8) in the shortest reaction times. Furthermore, within each series of catalysts no significant effect of the nature of the halide was observed. Finally, less than 20% yield of triazole was obtained in blank experiments carried out with copper halide salts CuX (X = Cl, Br and I) as catalysts in the absence of any phosphine ligand (entries 10-12). It is important to note that no sign of oxidation or disproportionation of any of the Cu(I) complexes was observed during the catalysts screening, even though the reaction were performed in aqueous media and under aerobic conditions. This observation underlines the effective protection imparted by terphenyl phosphine ligands to the Cu(I) centre during the catalysis.

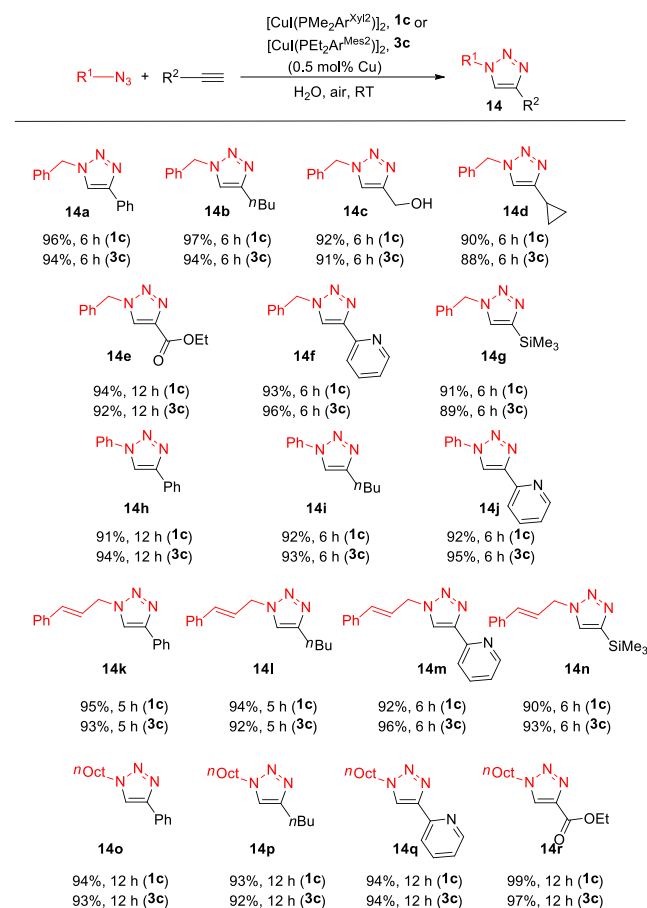**Table 3. Catalytic Performance of Complexes 1-5 in the [3+2] Cycloaddition of Benzyl Azide and Phenyl Acetylene.**[a]
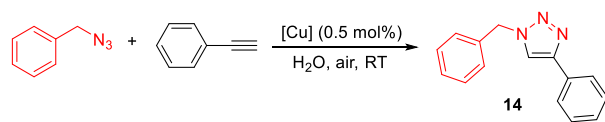
entry	[Cu]	time (h)	Yield (%)[b]
1	**1a**	6	92
2	**1b**	6	96
3	**1c**	6	96
4	**2a**	20	58
5	**2b**	20	55
6	**3a**	6	92
7	**3b**	6	97
8	**3c**	6	95
9	**5a**	20	62
10	CuCl	6	20
11	CuBr	6	16
12	CuI	6	16

[a]Reaction conditions: benzyl azide (1mmol), phenyl acetylene (1 mmol), Cu catalyst (0.005 mmol of Cu), H$_2$O (3 mL) under air. [b]Isolated yields (average of two runs).

To study the scope of the reaction complexes **1c** and **3c** were selected as the catalysts, since the these two Cu(I) iodide derivatives exhibited the best long-term air stability of each series. As shown in Table 4, a variety of azides and alkynes were smoothly converted into the corresponding triazoles in excellent yields under the reaction conditions. Benzyl, cynnamyl and phenyl azides reacted in short reaction times (5-6 h), whereas the alkyl-substituted *n*-octyl azide required longer reaction time (12 h) to reach completion (**14o-14r**). Conversely, the outcome was largely unaffected by the substituents on the terminal alkynes. Thus, aryl, alkyl, heteroaryl (pyridine), carboxylate and hydroxyl groups were equally well tolerated (see for example **14a-14g**).
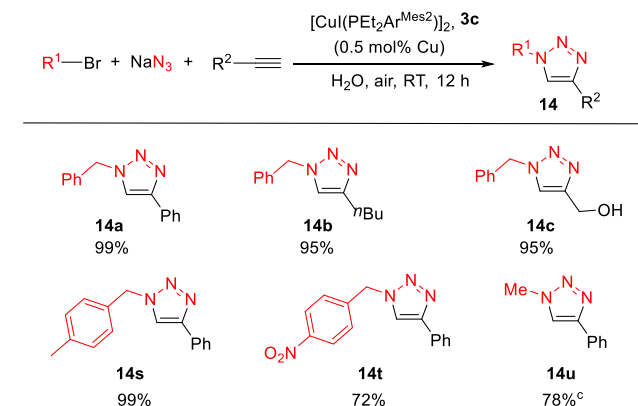
Organic azides, particularly those of low molecular weight or with high nitrogen content, are potentially explosive.[46] Therefore, various protocols that make use of *in situ* generated azides for the preparation of triazoles have been reported in the literature.[47] Given that most of the azides employed in this work were prepared from the reaction of alkyl halides with NaN$_3$, the activity of catalysts **1c** and **3c** were examined in the three-component reaction of benzyl bromide, NaN$_3$ and phenyl acetylene using the same reaction conditions as those described above for the reactions with the preformed azides. Under these conditions, only catalyst **3c** provided the triazole in quantitative yield, although in extended reaction time when compared with the reaction carried out with the isolated benzyl azide. The versatility of catalyst **3c** for the synthesis of triazoles by the three-component reaction of alkyl halides, NaN$_3$ and 1-alkynes is illustrated in Table 5. In all instances, the triazoles were obtained in good to high yields under otherwise unaltered reaction conditions. It is interesting to note that only very few Cu-based catalyst systems accomplished the one-pot synthesis of triazoles with such a low catalyst loading.[29c,48]

Table 4. Scope of Cycloaddition Reactions of Azides and Alkynes Catalyzed by Complexes 1c and 3c.[a,b]

R^1—N_3 + R^2—≡ $\xrightarrow[\text{H}_2\text{O, air, RT}]{\substack{[\text{CuI(PMe}_2\text{Ar}^{\text{Xyl2}})]_2, \textbf{1c} \text{ or}\\ [\text{CuI(PEt}_2\text{Ar}^{\text{Mes2}})]_2, \textbf{3c}\\ (0.5 \text{ mol\% Cu})}}$ **14** R^2

14a	**14b**	**14c**	**14d**
96%, 6 h (**1c**)	97%, 6 h (**1c**)	92%, 6 h (**1c**)	90%, 6 h (**1c**)
94%, 6 h (**3c**)	94%, 6 h (**3c**)	91%, 6 h (**3c**)	88%, 6 h (**3c**)

14e	**14f**	**14g**
94%, 12 h (**1c**)	93%, 6 h (**1c**)	91%, 6 h (**1c**)
92%, 12 h (**3c**)	96%, 6 h (**3c**)	89%, 6 h (**3c**)

14h	**14i**	**14j**
91%, 12 h (**1c**)	92%, 6 h (**1c**)	92%, 6 h (**1c**)
94%, 12 h (**3c**)	93%, 6 h (**3c**)	95%, 6 h (**3c**)

14k	**14l**	**14m**	**14n**
95%, 5 h (**1c**)	94%, 5 h (**1c**)	92%, 6 h (**1c**)	90%, 6 h (**1c**)
93%, 5 h (**3c**)	92%, 5 h (**3c**)	96%, 6 h (**3c**)	93%, 6 h (**3c**)

14o	**14p**	**14q**	**14r**
94%, 12 h (**1c**)	93%, 12 h (**1c**)	94%, 12 h (**1c**)	99%, 12 h (**1c**)
93%, 12 h (**3c**)	92%, 12 h (**3c**)	94%, 12 h (**3c**)	97%, 12 h (**3c**)

[a]Reaction conditions: azide (1mmol), 1-alkyne (1 mmol), Cu catalyst (0.5 mol% Cu), H_2O (3 mL) under air. [b]Isolated yield base on azide (average of two runs)

Table 5. Scope of Three-Component Reactions of Aryl Halides, NaN_3 and 1-Alkynes Catalyzed by Complex 3c.[a,b]

R^1—Br + NaN_3 + R^2—≡ $\xrightarrow[\text{H}_2\text{O, air, RT, 12 h}]{\substack{[\text{CuI(PEt}_2\text{Ar}^{\text{Mes2}})]_2, \textbf{3c}\\ (0.5 \text{ mol\% Cu})}}$ **14** R^2

14a	**14b**	**14c**
99%	95%	95%

14s	**14t**	**14u**
99%	72%	78%[c]

[a]Reaction conditions: alkyl halide (1 mmol), NaN_3 (1.3 mmol), 1-alkyne (1 mmol), catalyst **3c** (0.5 mol% Cu), H_2O (3 mL). [b]Isolated yields (average of two runs). [c]With MeI

5-yodo-1,2,3-triazoles are versatile intermediates for further functionalization via the halogen substituent.[49] However, there are still a limited number of efficient Cu-based catalyst systems for the CuAAC reactions between organic azides and 1-iodo alkynes.[29c,48,50] This prompted us to investigate the behavior of complexes **1c** and **3c** in this challenging transformation. Benzyl azide and iodoethynylbenzene were chosen as the model system. All reactions were conducted in water at room temperature under air and with 0.5 mol% [Cu]. Neither of the two Cu(I) catalyst was active under these conditions (Table 6, entries 1 and 2). Changing the solvent to THF or increasing the catalyst loading up to 5 mol% did not produced any significant improvement in the reaction yield (entries 3 and 5). The addition of nitrogen bases has been reported to be beneficial in these reactions.[48,50] Thus, by performing the cycloaddition in the presence of 4 mol% of 2,6-lutidine high yields of the 5-iodotriazole was obtained with both catalyst (entries 6 and 7). However, catalyst **3c** was less selective since small amounts of dehalogenated 5-H-triazol were also observed. No change either in yield or in selectivity was observed when the reactions were carried out under neat conditions (entries 8 and 9).

Table 6. Screening of reaction conditions for the cycloaddition between benzyl azide and iodoethynylbenzene catalyzed by complexes 1c and 3c.[a]

entry	catalyst	cat. loading (mol% Cu)	solvent	additive	Yield (%)[b]
1	1a	0.5	H_2O	-	Trace
2	3c	0.5	H_2O	-	Trace
3	1a	0.5	THF	-	Trace
4	3c	0.5	THF	-	Trace
5	3c	5	THF	-	20%
6	1a	1	H_2O	2,6-lutidine	>95
7	3c	1	H_2O	2,6-lutidine	90[c]
8	1a	1	neat	2,6-lutidine	>95
9	3c	1	neat	2,6-lutidine	90[c]

[a]Reaction conditions: benzyl azide (0.5 mmol), iodoethynylbenzene (0.5 mmol), solvent (3 mL), 24 h. [b]Determined by ^{1}H NMR with an internal standard. [c]5-10% of 5H-triazole was formed.

The optimized reaction conditions were then applied to different azides and 1-iodoalkynes giving the products 1,4-disubstituted 5-iodo-1,2,3-triazoles with the yields in the range of 45–95% (Table 7). n-octyl azide was the less reactive; consequently, reactions involving this azide were performed under neat conditions to obtain the products in moderate to good yields (**15c** and **15f**). Only

in the case of the cycloaddition of benzyl azide and iodoethynyl-cyclopropane, trace amounts of the dehalogenated triazol were detected (**15d**).

Table 7. Scope of Cycloaddition Reaction s of Azides and 1-Iodoalkynes Catalyzed by 1c.[a,b]
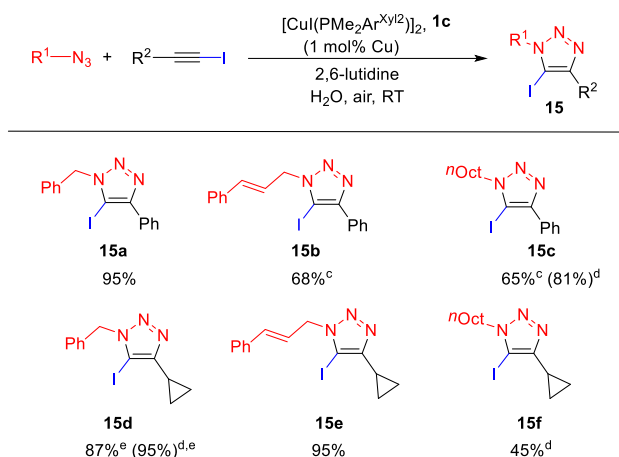
[a]Reaction conditions: azide (0.5 mmol), iodoethynylbenzene (0.5 mmol), catalyst **1c** (1 mol% Cu), H_2O (3 mL), 24 h. [b]Isolated yields (average of two runs). [c]With 2 mol% of Cu. [d]Neat. [e]Trace amounts of 5-H-triazole detected by ^{1}H NMR.

CONCLUSIONS

A family of Cu(I) halide complexes stabilized by dialkyl terphenyl phosphines, PR_2Ar', has been prepared and characterized. X-ray diffraction studies disclosed a bimetallic dihalo-bridged structure for compounds $[CuX(PR_2Ar')]_2$ with a distorted trigonal planar geometry at the metal centre and, in most cases, a C_{2h}-like symmetry. The presence of a Cu-Cu bond was detected for two iodide derivatives with an intermetallic distance of *ca*. 2.7 Å. Compounds $[CuI(PMe_2Ar^{Xyl2})]_2$ **1c** and $[CuI(PEt_2Ar^{Mes2})]_2$ **3c** behave in the same way in degassed liquid solution at 300 K (none of the two complexes is emissive), in solid-solid solution, *i.e.* Zeonex films, in the solid state at 77 K and in frozen cyclohexane solution(both complexes are emissive). In microcrystalline powder samples with sufficient rigid structure and order, however, the radiative relaxation of excited states is highly conditioned by interactions with adjacent molecules at room temperature. In such a way that just by blocking very specific vibrational modes at dimeric core site it is possible to "turn on" the emission at room temperature. In this study the centrosymmetric structure of complexes allowed the identification of such non-radiative deactivation vibrational modes and showed how structural knowledge can influence the design of novel luminescent Cu(I) complexes in the future. Among the dinuclear Cu(I) complexes prepared, $[CuI(PMe_2Ar^{Xyl2})]_2$ **1c** and $[CuI(PEt_2Ar^{Mes2})]_2$ **3c** are efficient catalysts for [3+2] cycloaddition of azides and terminal alkynes. Catalytic cycloadditons are conducted in water under air using low catalysts loadings. Remarkably, these conditions are compatible with the use of 1-iodoalkynes, a substrate scarcely used in Cu-AAC reactions.

EXPERIMENTAL SECTION

All preparations and manipulations were carried out under oxygen-free nitrogen, using conventional Schlenk techniques. Solvents were rigorously dried and degassed before use. Ligands **L1**-**L5**,[30a,31a] organic azides[51] and iodoalkynes[50a] were synthesized following previously reported procedures. Reagents were purchased from commercial suppliers and used without further purification. NMR spectra were recorded on Bruker Avance DPX-300, Avance DRX-400, Avance DRX-500, and 400 Ascend/R spectrometers. The ^{1}H and ^{13}C resonances of the solvent were used as the internal standard and the chemical shifts are reported relative to TMS while ^{31}P was referenced to external H_3PO_4. Elemental analyses were performed by the Servicio de Microanálisis of Instituto de Investigaciones Químicas (IIQ). CITIUS. X-ray diffraction studies were accomplished at Centro de Investigación Tecnología e Innovación, CITIUS (Universidad de Sevilla) and Centro de Investigación en Química Sostenible, CIQSO (Universidad de Huelva). Diffuse reflectance spectra were acquired in a Shimadzu UV-2501PC equipped with an integrating sphere. The powdered samples were smashed between two quartz lamellae, accommodated on a $BaSO_4$ filled support and the spectra run using an identical $BaSO_4$ filled support as blank. The remission function, F(R), was calculated using the Kubelka–Munk equation for optically thick samples. UV–vis absorbance spectra were acquired on a UV–vis–NIR Varian Cary 5000 spectrophotometer and fluorescence spectra were recorded on a SPEX Fluorolog-3 Model FL3–22 spectrofluorimeters. Time-resolved emission spectra were acquired in the same apparatus, using a pulsed xenon lamp with a full-width of 3 μs. Spectra and decays were collected with a minimum 50 μs delay to remove any interference from the lamp. Luminescence quantum efficiencies were measured by the absolute method with an Integrated Sphere. Films for optical characterization were prepared in zeonex (10% in toluene) matrix by drop-casting onto a quartz substrate with an emitter concentration of 1% (m/m). The Raman analysis was carried out using a Labram 300 Jobin Yvon spectrometer, equipped with a HeNe laser 17mW operating at 633 nm. The laser beam was focused with a 50x Olympus objective lens. The laser power at the surface of the samples was varied with the aid of a set of neutral density filters (D 0.6). DFT calculations have been carried out with the program Gaussian 09 using the B3LYP functional, 6-31G** basis set for C, H and a standard double-ζ polarized basis set, namely, the LANL2DZ set for Cu, I and P augmented with polarization functions on P (a d orbital with exponent 0.364 for P, upon EMSL basis set exchange database) For Cu, P and I we applied also Effective Core Potentials. Geometry optimization and TD-DFT calculations were performed in cyclohexane with the PCM solvation method. Molecular Orbital visualisation for all the complexes was performed using Avogadro 1.2.0.

Synthesis of [CuCl(PMe_2Ar^{Xyl2})] 1a. A mixture of the ligand PMe_2Ar^{Xyl}, **L1**, (0.080 g, 0.231 mmol) and CuCl (0.023 g, 0.231 mmol) in CH_2Cl_2 (5 mL) was stirred at room temperature for 20 h. After filtration, the resulting solution was evaporated to dryness affording **1a** as colorless solid. Yield: 0.098 g, 98%. ^{1}H NMR (300 MHz, $CDCl_3$): δ 7.57 (t, $^3J_{HH}$ = 7.6 Hz, 1H, p-C_6H_3), 7.30 (t, 2H, p-Xyl), 7.18 (d, $^3J_{HH}$ = 7.6 Hz, 4H, m-Xyl), 7.07 (dd, $^3J_{HH}$ = 7.6 Hz, $^4J_{HP}$ ~ 1 Hz, 2H, m-C_6H_3), 2.05 (s, 12 H, CH_3-Xyl), 1.14 (d, $^2J_{HP}$ = 6.8 Hz, 6H, P-CH_3).^{13}C NMR (75 MHz, $CDCl_3$): δ 147.1 (br s, o-C_6H_3), 140.2 (br s, *ipso*-Xyl), 135.4 (o-Xyl), 131.8 (p-C_6H_3),

130.5 (d, $^3J_{CP}$ = 6 Hz, m-C$_6$H$_3$), $ipso$-C$_6$H$_3$ masked by more intense signals, 128.7 (m-Xyl), 128.6 (p-Xyl), 21.5 (CH$_3$-Xyl), 14.0 (d, $^1J_{CP}$ = 23 Hz, P-CH$_3$). ^{31}P{^{1}H} NMR (121 MHz, CDCl$_3$): δ 34.3 (br s). Elemental analysis calculated (found) for C$_{48}$H$_{54}$Cu$_2$Cl$_2$P$_2$: C 64.71 (64.5), H 6.11 (6.2).

General catalytic procedure for the [3+2] cycloaddition of azides and terminal alkynes. Procedure A. A vial fitted with a screw cap was loaded with the alkyne (1 mmol), the azide (1 mmol), the copper complex (0.5 mol% Cu) and water (3 mL) under air. The reaction mixture was stirred at room temperature for 5-12 h. The product was extracted with ethyl acetate, the combined organic layers were washed with brine, dried over anhydrous MgSO$_4$ and the solvent was removed under vacuum. When required, the product was purified by flash column chromatography.

General catalytic procedure for the [3+2] cycloaddition of in situ generated azides and terminal alkynes. Procedure B. A vial fitted with a screw cap was loaded with the alkyne (1 mmol), the aryl halide (1 mmol), sodium azide (1.3 mmol), the copper complex (0.5 mol% Cu) and water (3 mL) under air. The reaction mixture was stirred at room temperature for 5-12 h. The product was extracted with ethyl acetate, the combined organic layers were washed with brine, dried over anhydrous MgSO$_4$ and the solvent was removed under vacuum. When required, the product was purified by flash column chromatography.

General procedure for the [3+2] cycloaddition of azides and iodoalkynes. In a vial fitted with a screw cap, the catalyst **1c** (1-2 mol%) was added to a mixture of iodoalkyne (1 mmol), 2,6-lutidine (4 mol%) and azide (1 mmol) in water (3 mL) under air. The reaction mixture was stirred at room temperature for 24 h. Then, the reaction was quenched by adding aqueous NH$_4$OH (1 mL, 10% solution). The volatile components were removed by evaporation, and the crude residue was extracted with diethyl ether and washed with water. The solvent was removed under vacuum and the product was purified by flash column chromatography.

ASSOCIATED CONTENT

Supporting Information Available. Experimental details, analytical, spectroscopic and crystal data, figures and tables. "This material is available free of charge via the Internet at http://pubs.acs.org."

Accession codes

CCDC 2001229-2001231, 2001348, 2001349, 2001351, 2001352 and 2003447 contain the supplementary crystallographic data for this paper. These data can be obtained free for charge from The Cambridge Crystallographic Data Centre via www.ccdc.cam.ac.uk/data_request/cif or by contacting The Cambridge Crystallographic Data Centre, 12 Union Road, Cambridge CB2 1EZ, UK; fax: +44 1223 336033.

AUTHOR INFORMATION

Corresponding Author

*E-mail: mnicasio@us.es (MCN); m.hosseinzadeh@campus.fct.unl.pt (MO); rpeloso@us.es (RP)

ORCID

M. Carmen Nicasio: 0000-0002-6485-2953

Mani Outis: 0000-0003-1940-8703

Riccardo Peloso: 0000-0002-9532-7609

REFERENCES

(1) Peng, R.; Li, M.; Li, D. Copper(I) Halides: A Versatile Family in Coordination Chemistry and Crystal Engineering. *Coord. Chem. Rev.* **2010**, *254*, 1-18.

(2) (a) Churchill, M. R.; Kalkra, K. L. Molecules with an M$_4$X$_4$ Core. III. Comparison of the X-ray Crystallographically Determined Molecular Structures of Tetrameric Triethylphosphinecopper(I) Iodide and Triethylarsinecopper(I) Iodide. *Inorg. Chem.* **1974**, *13*, 1899-1904; (b) Churchill, M. R.; DeBoer, B. G.; Mendak, S. J. Molecules with an M$_4$X$_4$ core. V. Crystallographic Characterization of the Tetrameric Cubane-Like Species Triethylphosphinecopper(I) Chloride and Triethylphosphinecopper(I) Bromide. Systematics in the [PEt$_3$CuX]$_4$ Series *Inorg. Chem.* **1975**, *14*, 2041-2047.

(3) Churchill, M. R.; Rotella, F. J. Molecules with an M$_4$X$_4$ core. 9. Crystal Structure and Molecular Geometry of Tetrameric (Methyldiphenylphosphine)Copper(I) Iodide, [(PMePh$_2$)CuI]$_4$. *Inorg. Chem.* **1977**, *16*, 3267-3273.

(4) (a) Barron, P. F.; Dyason, J. C.; Engelhardt, J. M.; Healy, P. C.; White, A. H. Lewis Base Adducts of Group IB Metal Compounds. 8. High-Resolution Solid-State Phosphorus-31 Nuclear Magnetic Resonance Spectra of Tetrameric ((Triphenylphosphine)Copper(I) Halide) Complexes and Crystal Structure Determination of "Cubane" [PPh$_3$CuBr]$_4$. *Inorg. Chem.* **1984**, *23*, 3766-3769; (b) Dyason, J. C.; Healy, P. C.; Engelhardt, L. M.; Pakawatchai, C.; Patrick, V. A.; Raston, C. L.; White, A. H. Lewis-base Adducts of Group 1 B Metal(I) Compounds. Part 16." Synthesis, Structure, and Solid-state Phosphorus-31 Nuclear Magnetic Resonance Spectra of some Novel [Cu$_4$X$_4$L$_4$] (X = Halogen, L = N, P Base) 'Cubane' Clusters. *J. Chem. Soc., Dalton Trans.* **1985**, 831-838.

(5) (a) Churchill, M. R.; Kalra, K. L. Molecules with an M$_4$X$_4$ core. II. X-ray Crystallographic Determination of the Molecular Structure of Tetrameric Triphenylphosphinecopper(I) Bromide in

Crystalline [PPh₃CuBr]₄·2CHCl₃. *Inorg. Chem.* **1974**, 13, 1427-1434; (b) Churchill, M. R.; DeBoer, B. G.; Donovan, D. J. Molecules with an M₄X₄ core. IV. Crystallographic Detection of a Step Configuration for the Molecules with an M4X4 Core. IV. Crystallographic Detection of a "Step" Configuration for the Cu₄I₄ Core in Tetrameric Triphenylphosphinecopper(I) Iodide, [PPh₃CuI]₄. *Inorg. Chem.* **1975**, 14, 617-623.

(6) (a) Churchill, M. R.; Rotella, F. J. Molecules with an M₄X₄ Core. Failure of the 1:1:1 Tricyclohexylphosphine-Copper(I)-Chloride Complex to Form a Tetramer. Crystal Structure of Dimeric (Tricyclohexylphosphine)copper(I) Chloride, [(P(cHx)₃)CuC1]₂. *Inorg. Chem.* **1979**, 18, 166-171; (b) Sloveichik, G. L.; Eisenstein, O.; Poulton J. T.; Streib, W. E.; Huffman, J. C.; Caulton, K. G. Multiple Structural Variants of LₙCuᴵ(μ-X)₂CuᴵLₙ (n = 1, 2). Influence of Halide on a "Soft" Potential Energy Surface. *Inorg. Chem.* **1992**, 31, 3306-3312.

(7) (a) Ramaprabhu, S.; Amstutz, N.; Lucken, E. A. C.; Bernardinelli, G. Copper-63,65 Nuclear Quadrupole Resonance of Complexes of Copper(I) Halides with Phosphorus-containing Ligands. *J. Chem. Soc., Dalton Trans.* **1993**, 871-875; (b) Bowmaker, G. A.; Hanna, J. V.; Hart, R. D.; Healy, P. C.; Skelton, B. W.; White, A. H. Structural and Spectroscopic Studies on the Dimeric Complexes of Tris(2-methylphenyl)phosphine With Copper(I) Halides. *Aust. J. Chem.* **1994**, 47, 25-45.

(8) (a) Ainscough, E. W.; Brodie, A. M.; Burrell, A. K.; Freeman, G. H.; Jameson, G. B.; Bowmaker, G. A.; Hanna, J. V.; Healy, P. C. Structural and Spectroscopic Studies on Three- and Two-co-ordinate Copper(I) Halide Tribenzylphosphine Complexes. *J. Chem. Soc., Dalton Trans.* **2001**, 144-151; (b) Bowmaker, G. A.; Boyd, S. E.; Hanna, J. V.; Hart, R. D.; Healy, P. C.; Skelton, B. W.; White, A. H. Structural and Spectroscopic Studies on Three-coordinate Complexes of Copper(I) Halides with Tricyclohexylphosphine. *J. Chem. Soc., Dalton Trans.* **2002**, 2722-2730.

(9) (a) Bowmaker, G. A.; Camp, D.; Hart, R. D.; Healy, P. C.; Skelton, B. W.; White, A. H. Comparative Structural Studies on Three-Coordinate Copper(I) Halide Complexes With Tertiary Phosphines. Crystal Structures of [(PPh₂Mes)CuX]₂ and [(PPhMes₂)CuX]₂ (Mes = Mesityl X = Cl, Br, I), *Aust. J. Chem.* **1992**, 45, 1155; (b) Zink, D. M.; Grab, T.; Baumann, T.; Nieger, M.; Barnes, E. C.; Klopper, W.; Bräse, S. Experimental and Theoretical Study of Novel Luminescent Di-, Tri-,and Tetranuclear Copper Triazole Complexes, *Organometallics* **2011**, 30, 3275; (c) Shou, R.-E.; Chai, W.-X.; Song, L.; Qin, L.-S.; Shi, H.-S.; Wang, T.-G. Three Luminescent Copper(I) Iodide Clusters with Phosphine Ligands: Synthesis, Structure Characterization, Properties and TD-DFT Calculations, *J. Clust. Sci.* **2017**, 28, 2185-2203.

(10) Alyea, E. C.; Ferguson, G.; Malito, J.; Ruhl, B. L. Monomeric (Trimesitylphosphine)copper(I) Bromide. X-ray Crystallographic Evidence for the First Two-Coordinate Copper(I) Phosphine Halide Complex. *Inorg. Chem.* **1985**, 24, 3719-3720.

(11) (a) Bowmaker, G. A.; Cotton, J. D.; Healy, P. C.; Kildea, J. D.; Silong, S. B.; Skelton, B. W.; White, A. H. Solid-State ³¹P NMR, Far-IR, and Structural Studies on Two-Coordinate (Tris(2,4,6-trimethoxyphenyl)phosphine)copper(I) Chloride and Bromide. *Inorg. Chem.* **1989**, 28, 1462-1466; (b) Baker, L.-J.; Bowmaker, G. A.; Hart, R. D.; Harvey, P. J.; Healy, P. C.; White, A. H. Structural, Far-IR, and Solid State 31P NMR Studies of Two-Coordinate Complexes of Tris(2,4,6-trimethoxyphenyl) phosphine with Copper(I) Iodide. *Inorg. Chem.* **1994**, 33, 3925-3931.

(12) Blake, A. J.; Brooks, N. R.; Champness, N. R.; Hanton L. R.; Hubberstey, P.; Schröder, M. Copper(1) Halide Supramolecular Networks Linked by N-heterocyclic Donor Bridging Ligands. *Pure Appl. Chem.* **1998**, 70, 2351-2357.

(13) (a) Ford, P. C.; Cariati, E.; Bourassa, J. Photoluminiscense Properties of Multinuclear Copper(I) Compounds. *Chem. Rev.* **1999**, 99, 3625-; (b) Xu, H.; Chen, R.; Sun, Q.; Lai, W.; Su, Q.; Huang, W.; Liu, X. Recent Progress in Metal-Organic Complexes for

Optoelectronic Applications. *Chem. Soc. Rev.* **2014**, 43, 3259-3302; (c) Wallesch, M.; Volz, D.; Zink, D. M.; Schepers, U.; Nieger, M.; Baumann, T.; Bräse, S. Bright Coppertunities: Multinuclear Cuᴵ Complexes with N-P ligands and Their Applications. *Chem. Eur. J.* **2014**, 5, 1638-1645; (d) Kumar, S.; Mondal, D.; Balakrishna, M. S. Diverse Architectures and Luminescence Properties of Group 11 Complexes Containing Pyrimidine-Based Phosphine, N-((Diphenylphosphine)methyl)pyrimidin-2-amine, *ACS Omega* **2018**, 3, 16601-16614; (e) Choubey, B.; Radhakrishna, L.; Mague, J. T.; Balakrishna, M. S. Two Triazole-Based Phosphine Ligands Prepared via Temperature Mediated Li/H Exchange: CuI and AuI Complexes and Structural Studies, *Inorg. Chem.* **2016**, 55, 8514-8526; (f) Bhat, S. A.; Mague, J. T.; Balakrishna, M. S. Synthesis and structural characterization of copper(I) halide complexes containing bis(azol-1-yl)methane derived bisphosphines, *Inorg. Chim. Acta* **2016**, 443, 243-250.

(14) Maini, L.; Braga, D.;Mazzeoa, P.P.;Ventura, B. Polymorph and isomer conversion of complexes based on CuI and PPh₃ easily observed via luminescence. *Dalton Trans.*, **2012**, 41, 531–539.

(15) Benito,Q.;Le Goff, X.F.;Nocton, G.;Fargues, A.; Garcia, A.; Berhault, A; Kahlal, S.; Saillard, J. Y.; Martineau, C.; Trel̊bosc, J.; Gacoin, T.; Boilot, J. P.; Perruchas, S. Geometry Flexibility of Copper Iodide Clusters: Variability in Luminescence Thermochromism. *Inorg. Chem.* **2015**, 54, 4483−4494.

(16) Zhou, W.B.; Dong, Z.C.;Song, J.Li.;Zeng, H.Y.;Cao, R.;Guo, G.C.;Huang, J.S.;Li, J. Syntheses, Structures, Bonding, and Optical Properties of Trinuclear Cluster Iodides: M₃(μ₃-I)₂(μ-dppm)₃I (M=Cu, Ag, dppm=bis(diphenylphosphino)methane) *Journal of Cluster Science*, **2002**, 13, 119-136.

(17) Kang, L.;Chen, J;Teng, T.;Chen, X.L.;Yu, R.;Lu, C.Z. Experimental and theoretical studies of highly emissive dinuclear Cu(I) halide complexes with delayed fluorescence. *Dalton Trans.*, **2015**, 44, 11649–11659.

(18) Neese, F.;Solomon, E. I. Calculation of Zero-Field Splittings, g-Values, and the Relativistic Nephelauxetic Effect in Transition Metal Complexes. Application to High-Spin Ferric Complexes. *Inorg. Chem.* **1998**, 37, 6568-6582.

(19) Hofbeck, T.;Yersin, H. The Triplet State of fac-Ir(ppy)₃. *Inorg. Chem.*, **2010**, 49, 9290-9299.

(20) Norby, G.E.;Park, C.D.;O'Brien, B.;Li, G.;Huang, L.;Li, J. Efficient white OLEDs employing red, green, and blue tetradentate platinum phosphorescent emitters. *Organic Electronics*, **2016**, 37, 163-168.

(21) (a) Bhunia , S.; Pawar, G. G.; Kumar, S. V.; Jiang, Y.; Ma, D. Selected Copper-Based Reactions for C−N, C−O, C−S, and C−C Bond Formation. *Angew. Chem. Int. Ed.* **2017**, 56, 16136-16179; (b) Evano, G.; Blanchard, N.; Toumi, M. Copper-Mediated Coupling Reactions and Their Applications in Natural Products and Designed Biomolecules Synthesis. *Chem. Rev.* **2008**, 108, 3054-3131.

(22) McCann, S. D.; Stahl, S. S. Copper-Catalyzed Aerobic Oxidations of Organic Molecules: Pathways for Two-Electron Oxidation with a Four-Electron Oxidant and a One-Electron Redox-Active Catalyst. *Acc. Chem. Res.* **2015**, 48, 1756-1766.

(23) Hemming, D.; Fritzemeier, R.; Westcott, S. A.; Santos, W. L.; Steel, P. G. Copper-boryl Mediated Organic Synthesis. *Chem. Soc. Rev.* **2018**, 47, 7477-7494.

(24) (a) Díaz-Requejo, M. M.; Pérez, P. J. Coinage Metal Catalyzed C−H Bond Functionalization of Hydrocarbons. Chem. Rev. 2008, 108, 3379-3394; (b) Guo, X.-X.; Gu, D.-W.; Wu, Z.; Zhang, W. Copper-Catalyzed C–H Functionalization Reactions: Efficient Synthesis of Heterocycles. *Chem. Rev.* **2015**, 115, 1622-1651.

(25) (a) Meldal, M.; Tornøe, C. W. Cu-Catalyzed Azide−Alkyne Cycloaddition. *Chem. Rev.* **2008**, 108, 2952-3015; (b) E. Haldón,

M. C. Nicasio, P. J. Pérez. Copper-catalysed Azide–Alkyne Cycloadditions (CuAAC): an Update. *Org. Biomol. Chem*. **2015**, *13*, 9528-9550.

(26) Kolb, H. C.; Finn, M. G.; Sharpless, B. K. Click Chemistry: Diverse Chemical Function from a Few Good Reactions. *Angew. Chem. Int. Ed*. **2001**, *40*, 2004-2021.

(27) See for example: (a) Díez-González, S.; Correa, A.; Cavallo, L.; Nolan, S. P. (NHC)Copper(I)-Catalyzed [3+2] Cycloaddition of Azides and Mono- or Disubstituted Alkynes, *Chem. Eur. J*. **2006**, *12*, 7558-7564; (b) Díez-González, S.; Stevens, E. D.; Nolan, S. P. A [(NHC)CuCl] complex as a latent Click catalyst, *Chem. Commun*. **2008**, 4747-4749; (c) Díez-González, S.; Nolan, S. P. [(NHC)₂Cu]X Complexes as Efficient Catalysts for Azide–Alkyne Click Chemistry at Low Catalyst Loadings. *Angew. Chem. Int. Ed*. **2008**, *47*, 8881; (d) Jin, L.; Romero, E. A.; Melaimi, M.; Bertrand, G. The Janus Face of the X Ligand in the Copper-Catalyzed Azide-Alkyne Cycloaddition. *J. Am. Chem. Soc*. **2015**, *137*, 50, 15696-15698; (e) Bidal, Y. D.; Lesieur, M.; Melaimi, M.; Nahra, F.; Cordes, D. B.; Arachchige, K. S. A.; Slawin, A. M. Z.; Bertrand, G.; Cazin, C. S. J. Copper(I) Complexes Bearing Carbenes Beyond Classical N-Heterocyclic Carbenes: Synthesis and Catalytic Activity in "Click Chemistry". *Adv. Synth. Catal*. **2015**, *357*, 3155-3161.

(28) (a) Pérez-Balderas, F.; Ortega-Muñoz, M.; Morales-Sanfrutos, J.; Hernández-Mateo, F.; Calvo-Flores, F. G.; Calvo-Asín, J. A.; Isac-Garcilla, J.; Santoyo-González, F.; Multivalent Neoglycoconjugates by Regiospecific Cycloaddition of Alkynes and Azides Using Organic-Soluble Copper Catalysts. *Org. Lett*. **2003**, *5*, 1951-1954; (b) Méndez-Ardoy, A.; Gómez-García, M.; OrtizMellet, C.; Sevillano, N.; Girón, M. D.; Salto, R.; Santoyo-Gonzalez, F.; García-Fernández, J. M. Preorganized Macromolecular Gene Delivery Systems: Amphiphilic b-cyclodextrin "Click Clusters". *Org. Biomol. Chem*. **2009**, *7*, 2681-2684; (c) Wang, D.; Li, N.; Zhao, M.; Shi, W.; Ma, C.; Chen, B. Solvent-free Synthesis of 1,4-Disubstituted 1,2,3-Triazoles Using a Low Amount of Cu(PPh₃)₂NO₃ Complex. *Green Chem*. **2010**, *12*, 2120-2123; (d) Wang, D.; Zhao, M.; Liu, X.; Chen, Y.; Li, N.; Chen, B. Quick and Highly Efficient Copper-Catalyzed Cycloaddition of Organic Azides with Terminal Alkynes. *Org. Biomol. Chem*. **2012**, *10*, 229-231; (e) Gonda, Z.; Novák, Z. Highly Active Copper-Catalysts for Azide-Alkyne Cycloaddition. *Dalton Trans*. **2010**, *39*, 726-729.

(29) (a) Lal, S.; Díez-González, S. [CuBr(PPh₃)₃] for Azide-Alkyne Cycloaddition Reactions under Strict Click Conditions. *J. Org. Chem*. **2011**, *76*, 2367-2373; (b) Lal, S.; McNally, J.; White, A. J. P.; Díez-González, S. Novel Phosphinite and Phosphonite Copper(I) Complexes: Efficient Catalysts for Click Azide−Alkyne Cycloaddition Reactions. *Organometallics* **2011**, *30*, 6225-6232; (c) Pérez, J. M.; Crosbie, P.; Lal, S.; Díez-González, S. Copper(I)-Phosphinite Complexes in Click Cycloadditons: Three-Component Reactions and Preparation of 5-Iodotriazoles. *ChemCatChem* **2016**, *8*, 2222-2226.

(30) (a) Ortega-Moreno, L.; Fernández-Espada, M.; Moreno, J. J.; Navarro-Gilabert, C.; Campos, J.; Conejero, S.; López-Serrano, J.; Maya, C.; Peloso, R.; Carmona, E. Synthesis, Properties, and Some Rhodium, Iridium, and Platinum Complexes of a Series of Bulky m-Terphenylphosphine Ligands. *Polyhedron*, **2016**, *116*, 170-181; (b) Ortega-Moreno, L.; Peloso, R.; López-Serrano, J.; Iglesias Sigüenza, J.; Maya, C.; Carmona, E. A Cationic Unsaturated Platinum(II) Complex that Promotes the Tautomerization of Acetylene to Vinylidene, *Angew. Chem. Int. Ed*. **2017**, *56*, 2772-2775; (c) Ortega-Moreno, L., Peloso, R., Maya, C., Suárez, A., Carmona, E. Platinum(0) olefin complexes of a bulky terphenylphosphine ligand. Synthetic, structural and reactivity studies, *Chem. Commun*. **2015**, *51*, 17008-17011.

(31) (a) Marín, M.; J. Moreno, J.; Navarro-Gilabert, C.; Álvarez, E.; Maya, C.; Peloso, R.; Nicasio, M. C.; Carmona, E. Synthesis,

Structure and Nickel Carbonyl Complexes of Dialkylterphenyl Phosphines. *Chem. Eur. J*. **2019**, *25*, 260-272; (b) Marín, M.; Moreno, J. J.; Alcaide, M. M.; Álvarez, E.; López-Serrano, J.; Campos, J.; Nicasio, M. C.; Carmona, E. Evaluating Stereoelectronic Properties of Bulky Dialkylterphenyl Phosphine Ligands *J. Organomet. Chem*. **2019**, *896*, 120-128.

(32) (a) Campos, J. Dihydrogen and Acetylene Activation by a Gold(I)/Platinum(0) Transition Metal Only Frustrated Lewis Pair, *J. Am. Chem. Soc*. **2017**, *139*, 2944-2947; (b) Hidalgo, N; Bajo, S.; Moreno, J.J.; Navarro-Gilabert, C.; Mercado, B. Q.; Campos, J. Reactivity of a gold(i)/platinum(0) frustrated Lewis pair with germanium and tin dihalides, *Dalton Trans*. **2019**, *48*, 9127-9138 (c) Hidalgo, N.; Moreno, J.J.; Pérez-Jiménez, M.; Maya, C.; López-Serrano, J., Campos, J. Evidence for Genuine Bimetallic Frustrate Lewis Pair Activation of Dihydrogen with Gold(I)/Platinum(0) Systems, *Chem. Eur. J*. **2020**, doi.org/10.1002/chem.201905793.

(33) Zhang, S.; Zhao, L. A. A merged copper (I/II) cluster isolated from Glaser coupling, *Nat. Commun*. **2019**, *10*, 4848-4855.

(34) Cordero, B.; Gómez, V.; Platero-Prats, A. E.; Revés, M.; Echeverría, J.; Cremades, E.; Barragán, F.; Álvarez, S. Covalent radii revisited, *Dalton Trans*. **2008**, 2832-2838.

(35) For recent reviews on d^{10}-d^{10} interactions see for example: (a) Harisomayajula, N. V. S.; Makovetskyi, S.; Yi-Chou Tsai, Y.-C. Cuprophilic Interactions in and btween Molecular Entities, *Chem. Eur. J*. **2019**, *25*,936-954; (b) Sculfort, S.; Braunstein, P. Intramolecular d^{10}-d^{10} interactions in heterometallic clusters of the transition metals, *Chem. Soc. Rev*. **2011**, *40*, 2741-2760.

(36) Hofbeck, T.;Monkowius, U.;Yersin, H. Highly Efficient Luminescence of Cu(I) Compounds: Thermally Activated Delayed Fluorescence Combined with Short-Lived Phosphorescence. *J. Am. Chem. Soc*. **2015**, 137, 399−404.

(37) (a) Nozaki, K.; Iwamura, M. Highly Emissive d^{10} Metal Complexes as TADF Emitters with Versatile Structures and Photophysical Properties in *Highly Efficient OLEDs Materials Based on Thermally Activated Delayed Fluorescence*; Yersin H.; VCH: Weinheim, **2019**; pp 62-63. (b) Penfold, T.J.; Gindensperger, E.; Daniel, C.; Marian, C.M. Spin-Vibronic Mechanism for Intersystem Crossing. *Chem. Rev*. **2018**, 118, 6975−7025 (c) Li, E.Y.; Jiang, T.; Chib, Y.; Chou, P.T. Semi-quantitative assessment of the intersystem crossing rate: an extension of the El-Sayed rule to the emissive transition metal complexes. *Phys. Chem. Chem. Phys*. **2014**, 16, 26184-26192.

(38) (a) Eng, J.; Thompson, S.; Goodwin, H.; Credgington, D.; Penfold, T.J. Competition between the heavy atom effect and vibronic coupling in donor–bridge–acceptor organometallics. *Phys. Chem. Chem. Phys*. **2020**, 22, 4659-4667.(b) Baryshnikov, G.; Minaev, B.; Ågren, H. Theory and Calculation of the Phosphorescence Phenomenon. *Chem. Rev*. **2017**, 117, 6500-6537.

(39) (a) Jean, Y.; Voltaron, F. The fragment orbital method; application to some model systems in *An Introduction to Molecular Orbitals*; Brudett J. OXFORD UNIVERSITY PRESS: New York,1993; pp 126-127; (b) Pearson, R.G. Concerning Jahn-Teller Effects (first-order, pseudo, and second-order Jahn-Teller effects/symmetry rules). *Proc. Nat. Acad. Sci. USA* 72, **1975**, 2014-2016.

(40) (a) Paterson, M. J.; Bearpark, M. J.; Robb, M. A.; Blancafortc, L.; Worthd, G. A. Conical intersections: A perspective on the computation of spectroscopic Jahn-Teller parameters and the degenerate 'intersection space'. *Phys. Chem. Chem. Phys*. **2005**, 7, 2100-2215. (b) González, L.; Escudero, D.; Serrano-Andrés L. Progress and Challenges in the Calculation of Electronic Excited States. *ChemPhysChem*. **2012**, 13, 28–51. (c) Domcke, W.; Yarkony, D.R. Role of Conical Intersections in Molecular Spectroscopy and Photoinduced Chemical Dynamics. *Annu. Rev. Phys. Chem*. **2012**, 63, 325–352.

(41) (a) Chen, L. X.; Shaw, G.B.; Novozhilova, I.; Liu, T.; Jennings, G.; Attenkofer, K.; Meyer, G.J.; Coppens, P. MLCT State Structure and Dynamics of a Copper(I) Diimine Complex Characterized by Pump-Probe X-ray and Laser Spectroscopies and DFT Calculations. *J. AM. CHEM. SOC.* **2003**,125 , 7022-7034 (b) Iwamura, M.; Takeuchi, S.; Tahara, T. Real-Time Observation of the Photoinduced Structural Change of Bis(2,9-dimethyl-1,10-phenanthroline)copper(I) by Femtosecond Fluorescence Spectroscopy: A Realistic Potential Curve of the Jahn-Teller Distortion. *J. Am. Chem. Soc.* **2007**, 129, 5248-5256.(c) Iwamura, M.; Takeuchi, S.; Tahara, T. Ultrafast Excited-State Dynamics of Copper(I) Complexes. *Acc. Chem. Res.* **2015**, 48, 782−791.

(42) Krylova, V.A.; Djurovich, P.I; Aronson, J.W.; Haiges, R.; Whited, M.T.; Thompson, M.E. Structural and Photophysical Studies of Phosphorescent Three Coordinate Copper(I) Complexes Supported by an N-Heterocyclic Carbene Ligand. *Organometallics.* **2012**, 31, 7983-7993.

(43) (a) Fumanal, M.; Plasser. F.; Mai, S.; Chantal, D.; Gindensperger, G. Interstate vibronic coupling constants between electronic excited states for complex molecules. *J.Chem.Phys.* **2018**, 148,124119. (b) Neethu Anand. N.; Isukapalli. S.V.K.; Vennapusa, S.R. Excited-state intramolecular proton transfer driven by conical intersection in hydroxychromones. *J Comput Chem.* **2020**, 1–13. (c) Capano, G.; Penfold, T.J.; Röthlisberger, U.; Tavernellia, I. A Vibronic Coupling Hamiltonian to Describe the Ultrafast Excited State Dynamics of a Cu(I)-Phenanthroline Complex. *Chimia.* **2014**, 68, 227–230.

(44) (a) Zou, W.; Izotov, D.; Cremer. D. New Way of Describing Static and Dynamic Deformations of the Jahn-Teller Type in Ring Molecules. *J. Phys. Chem. A* **2011**, 115, 8731–8742. (b) D. Cremer. A General Definition of Ring Substituent Positions. *Israel Journal of Chemistry.* *1*980, 20, 12-19.

(45) (a) Kwon, E.; Kim, J.; Lee, K. Y.; Kim, T.H. Non-Phase-Transition Luminescence Mechanochromism of a Copper(I) Coordination Polymer. *Inorg. Chem.* **2017**, 56, 943−949; (b) Bowmaker, G. A.; Knappstein, R. J.; Tham, S.F. An Infrared and Raman Spectroscopic Study of Some Group 1B Halide Complexes Containing an M_4X_4 Core. *Aust. J. Chem.* **1978**, *31*, 2137-2143.

(46) Bräse, S.; Gil, C.; Knepper, K.; Zimmermann, V. Organic Azides: An Exploding Diversity of a Unique Class of Compounds. *Angew. Chem. Int. Ed.* **2005**, *44*, 5188-5240.

(47) Hassana, S.; Müllera, T. J. J. Multicomponent Syntheses Based Upon Copper-Catalyzed Alkyne-Azide Cycloaddition. *Adv. Synth. Catal.* **2015**, *357*, 617-666.

(48) García-Alvarez, J.; Díez, J.; Gimeno, J. A Highly Efficient Copper(I) Catalyst for the 1,3-Dipolar Cycloaddition of Azides with Terminal and 1-Iodoalkynes in Water: Regioselective Synthesis of 1,4-Disubstituted and 1,4,5-Trisubstituted 1,2,3-Triazoles. *Green. Chem.* **2010**, *12*, 2127-2130.

(49) See for example: Wei, F.; Wang, W.; Ma, Y.; Tunga, C-H.; Xu, Z. Regioselective Synthesis of Multisubstituted 1,2,3-Triazoles: Moving Beyond the Copper-Catalyzed Azide–Alkyne Cycloaddition. *Chem. Commun.* **2016**, *52*, 14188 and references therein.

(50) (a) Hein, J. E.; Tripp, J. C.; Krasnova, L. B.; Sharpless, K. B.; Fokin, V. V. Copper(I)-Catalyzed Cycloaddition of Organic Azides and 1-Iodoalkynes. *Angew. Chem. Int. Ed.* **2009**, *48*, 8018-8021; (b); Lal, S.; Rzepa, H. S.; Díez-González, S. Catalytic and Computational Studies of N-Heterocyclic Carbene or Phosphine-Containing Copper(I) Complexes for the Synthesis of 5-Iodo-1,2,3-Triazoles. *ACS Catal.* **2014**, *4*, 2274-2287; (c) Wang, D.; Chen, S.; Chen, B. 'Green' Synthesis of 1,4-Disubstituted 5-Iodo-1,2,3-Triazoles Under Neat Conditions, and an Efficient Approach of Construction of 1,4,5-Trisubstituted 1,2,3-Triazoles in One Pot. *Tetrahedron Lett.* **2015**, *55*, 7026-7028; (d) Chung, R.; Vo, A.; Fokin, V. V.; Hein, J. E. Catalyst Activation, Chemoselectivity, and Reaction Rate Controlled by the Counterion in the Cu(I)-Catalyzed Cycloaddition between Azide and Terminal or 1-Iodoalkynes. *ACS Catal.* **2018**, *8*, 7889-7897.

(51) (a) Alvarez, S. G.; Alvarez, M. T. A Practical Procedure for the Synthesis of Alkyl Azides at Ambient Temperature in Dimethyl Sulfoxide in High Purity and Yield. *Synthesis* 1997, 413-414. (b) Tao, C-Z.; Cui, X.; Li, J.; Liu, A-X.; Liu, L.; Guo, Q-X. Copper-Catalyzed Synthesis of Aryl Azides and 1-Aryl-1,2,3-Triazoles from Boronic Acids. *Tetrahedron Lett.* **2007**, *48*, 3525-3529. (c) Campbell-Verduyn, L.; Mirfeizi, L.; Dierckx, R. A.; Elsinga, P. H.; Feringa, B. L. Phosphoramidite Accelerated Copper(I)-Catalyzed [3+2] Cycloadditions of Azides and Alkynes. *Chem. Commun.* **2009**, 2139-2141.

SYNOPSIS TOC. A family of binuclear dihalo-bridged Cu(I) complexes stabilized with dialkyl terphenyl phosphine ligands have been synthesized and structurally characterized. Two phosphorescent complexes containing the Cu_2I_2 core, have been identified and their excited state dynamics where investigated. The novel compounds exhibit remarkable catalytic activities in CuAAC reactions performed in water under aerobic conditions.